Global and Local Nonlinear System Responses under Narrowband Random Excitations. II: Prediction, Simulation, and Comparison

Dongjun Yuk[1]; Solomon C. Yim, M.ASCE[2]; Arvid Naess, M.ASCE[3]; and I-Ming Shih[4]

Abstract: The response behavior of the single-degree-of-freedom (SDOF) nonlinear structural system subjected to narrowband stochastic excitations studied in Part I is investigated via simulations to verify the stochastic system characteristics assumed in the development of the semianalytical method. In addition, to demonstrate the accuracy of the method, predicted response–amplitude probability distributions are presented and compared to simulation results. Numerical simulations are conducted by directly integrating the SDOF system with the narrowband excitation modeled by the 1971 Shinozuka formulation. It is observed that the proposed semianalytical method is capable of accurately characterizing the stochastic response behavior of the nonlinear system by predicting the response–amplitude probability distribution and capturing the trends of variations in the response–amplitude statistical properties. In both the primary and the subharmonic resonance regions, good agreements between the response–amplitude probability distributions predicted by the semianalytical method and obtained from simulation results are observed both qualitatively and quantitatively. In addition, trends of the variations in the probability masses associated with the modes with variations in excitation parameters (bandwidth and variance) are captured.

DOI: XXXX

CE Database subject headings: Stochastic processes; Excitation; Simulation; Predictions; Parameters; Structural behavior.

Introduction

The response of a nonlinear oscillator under narrowband random excitation exhibits complex behavior including amplitude jump phenomena (global bifurcation), subharmonic response, superharmonic response, and even chaotic response (Nayfeh and Mook 1979; Guckenheimer and Holmes 1986). Knowledge of the behavior of a nonlinear oscillator can be utilized in various design application areas including structural, mechanical, and aerospace engineering, etc. To analyze these complex response behaviors, a semianalytical methodology is developed in Part I (Yim et al. 2006) based on the understanding of the nonlinear system response characteristics under deterministic excitations and the assumptions of a narrowband stochastic excitation. In addition, both the excitation–amplitude and the response–amplitude processes are approximated as stationary Markov processes. The attraction–domain transitions are modeled as a stationary Markov chain.

[1]Post-Doctoral Fellow, Dept. of Civil Engineering, Oregon State Univ., Corvallis OR 97331-2302.

[2]Professor, Dept. of Civil Engineering, Oregon State Univ., Corvallis OR 97331-2302 (corresponding author). E-mail: solomon.yim@orst.edu

[3]Professor, Dept. of Mathematics Sciences, Norwegian Univ. of Science and Technology, NO-7491 Trondheim, Norway.

[4]Formerly, Graduate Research Assistant, Dept. of Civil Engineering, Oregon State Univ., Corvallis OR 97331-2302.

Note. Associate Editor: Ross Barry Corotis. Discussion open until June 1, 2007. Separate discussions must be submitted for individual papers. To extend the closing date by one month, a written request must be filed with the ASCE Managing Editor. The manuscript for this paper was submitted for review and possible publication on December 19, 2005; approved on April 19, 2006. This paper is part of the ***Journal of Engineering Mechanics***, Vol. 133, No. 1, January 1, 2007. ©ASCE, ISSN 0733-9399/2007/1-1–XXXX/$25.00.

The formulation of the governing probability transition matrix developed in Part I is directly related to the excitation bandwidth and variance, as well as the amplitude jump phenomena of the nonlinear system. The probability of the system response being in an attraction domain can be obtained by solving the eigenvector of the probability transition matrix corresponding to the unit eigenvalue.

The governing equation for the response–amplitude perturbation probability within the response–amplitude domains corresponding to two excitation amplitudes is also formulated based on the Markov approximation. The transition probability density function depends on the system transient–state response characteristics as well as the excitation bandwidth and variance.

In this companion (Part II) study, the verification and calibration of the prediction capability of the semianalytical method developed and the numerical simulations based on Shinozuka (1971) and Shinozuka and Deodatis (1991) presented in Part I are conducted and compared with predictions from the proposed analysis method. The influences of varying excitation bandwidth and variance parameters on the response behavior are investigated. Furthermore, comparisons of the accuracy of prediction results by the proposed semianalytical method and two existing analytical methods, namely, stochastic averaging method (Roberts and Spanos 1986) and quasi-harmonic method (Lin and Yim 1997), are conducted against simulation histograms.

Stochastic Response Behavior

Jump Phenomenon (Global Bifurcation)

The system response under a narrowband excitation exhibits amplitude jumps between two distinct levels as shown in Fig. 1. To depict the mechanism of this global bifurcation behavior, an

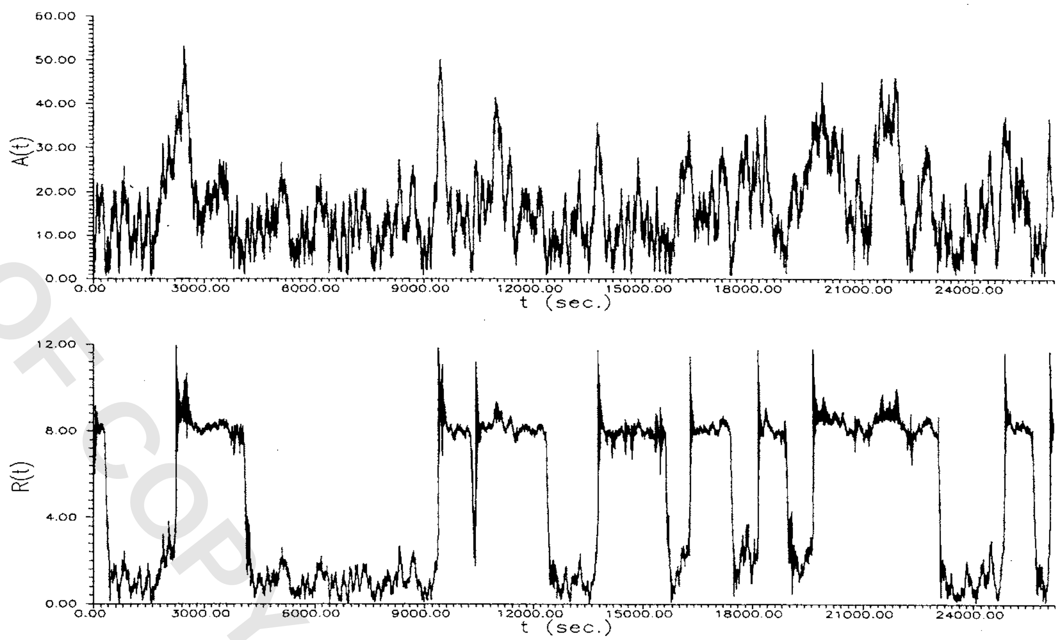

Fig. 1. System response in subharmonic resonance region. Time series of narrowband excitation amplitude (top) and corresponding response amplitude (bottom) (c_s=0.05, a_1=1, a_3=0.3, ω_f=3.6, σ_f^2=157, γ=0.005).

amplitude–response map is employed. The map is obtained by plotting the excitation amplitudes versus the corresponding measured response amplitudes, as shown in Fig. 2. In addition, the corresponding analytical response–amplitude curves of the system are presented as solid lines, in Fig. 2. It is revealed that the characteristics of the deterministic response attraction–domain transition behavior depicted in Part I is preserved under a narrowband excitation environment. Namely, the system response goes from the large-amplitude domain to the small-amplitude domain when the excitation amplitude varies from a value greater than to a value less than the large-amplitude domain lower boundary.

Subharmonic Responses

An examination of the details of response time series (e.g., Fig. 1) reveals the repeated occurrence of 1/2 and 1/3 subharmonic responses under narrowband excitations. For the system with parameters given in Fig. 1, the system response oscillates at two distinct amplitude levels. These subharmonic responses are often difficult to identify due to overlapping of the different response amplitude domains among the small amplitude, 1/2 and 1/3 subharmonic domains. However, the existence of these responses can be identified relatively clearly in the associated amplitude response maps (e.g., Fig. 2) by observing the significant number of points located along the analytical subharmonic amplitude–response curves (shown as the solid lines).

From the response–amplitude maps, it is observed that the system response may enter the 1/2 or the 1/3 subharmonic domain when an exit from the large amplitude harmonic domain occurs. As a result, the subharmonic responses may occur repeatedly, although the duration of stay in each visit of the system response in these domains may be relatively short. Note that the existence of the 1/3 subharmonic response under narrowband excitation was also observed in simulations conducted in previous studies (Davies and Nandall 1986; Davies and Rajan 1988; Rajan and Davies 1988; Davies and Liu 1990; Francescutto 1991) when an extremely small excitation bandwidth parameter and special system initial conditions are employed. However, it was concluded that the 1/3 subharmonic response only exists in the beginning of a response realization, and once it disappears, it would not be observed again. The contradiction in the observation of repeated occurrence of the subharmonic response in this study and the predictions in the literature may be due to different simulation durations employed. In this study, the simulation duration is on the order of 12,000 excitation cycles, significantly longer than the 600 cycles employed in previous studies.

Frequency of Occurrence

Stochastic system response characteristics, including transition among various attraction domains (global bifurcation) and fre-

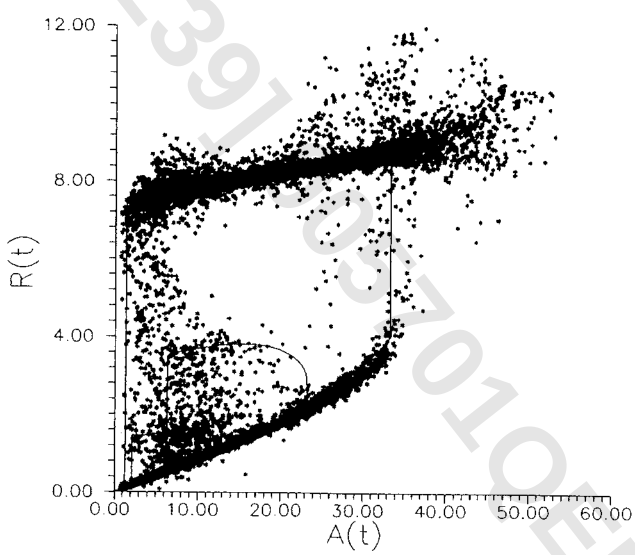

Fig. 2. Response–amplitude maps corresponding to time series shown in Fig. 1

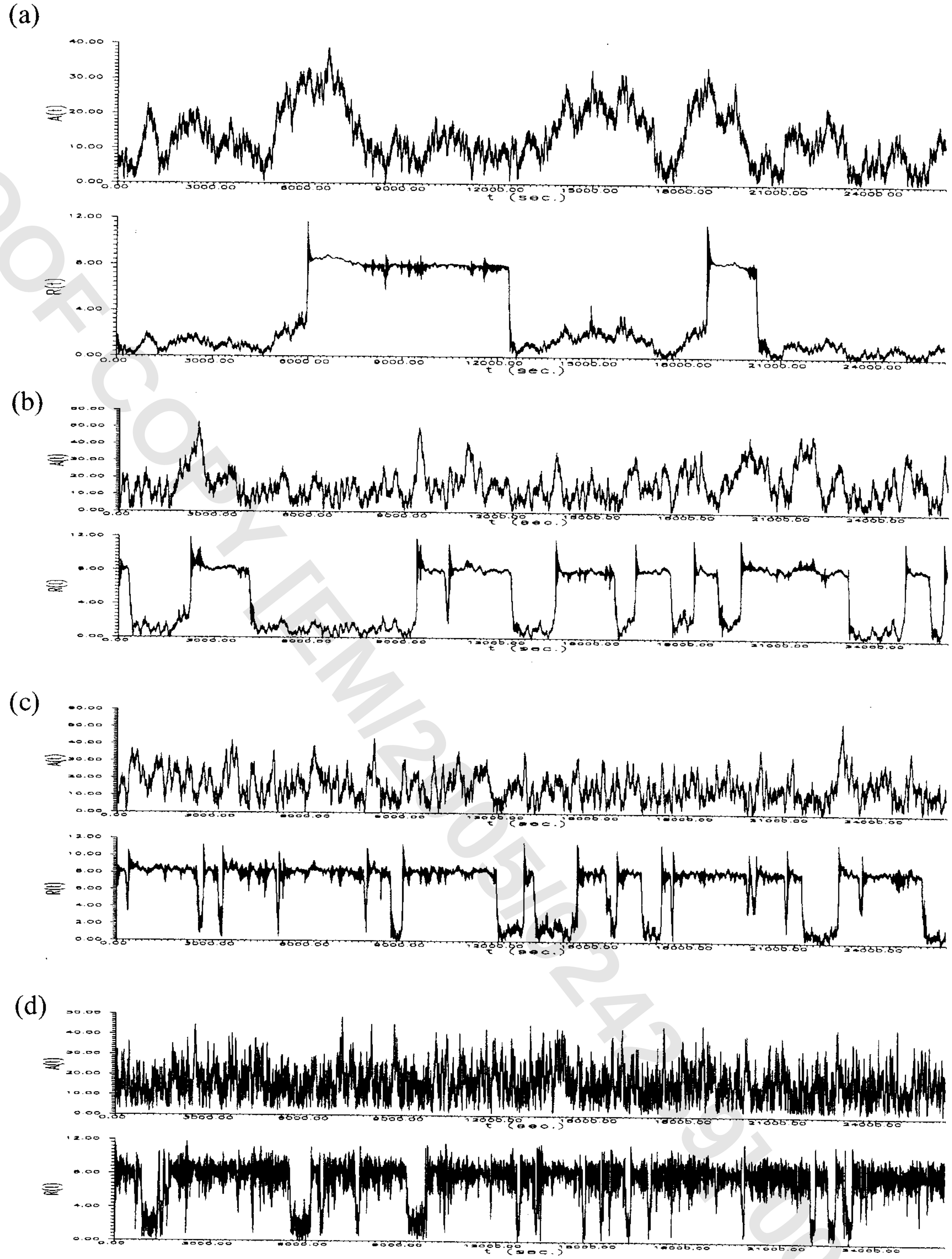

Fig. 3. (a, b, c, and d) System response under varying excitation bandwidths in subharmonic resonance region. Time series of narrowband excitation amplitude (top) and corresponding response amplitude (bottom) [c_s=0.05, a_1=1, a_3=0.3, ω_f=3.6, σ_f^2=157, γ=(a) 0.001; (b) 0.005; (c) 0.01; (d) 0.05].

quency of occurrence can be observed in the time histories and response–amplitude maps. The frequencies of occurrence in these maps are found to be attraction-domain dependent. As indicated in Figs. 1 and 2, the frequencies of occurrence are relatively high for both large and small amplitude harmonic responses, and low for the 1/2 and 1/3 subharmonic responses. Note that the randomness in the excitation is independent of the attraction domain. This indicates the dependency of the response–amplitude perturbation behavior on the system characteristics and the attraction domains.

Effect of Varying Excitation Bandwidth

The effects of varying the degree of randomness of the excitation (i.e., excitation bandwidth) on the response behavior are demon-

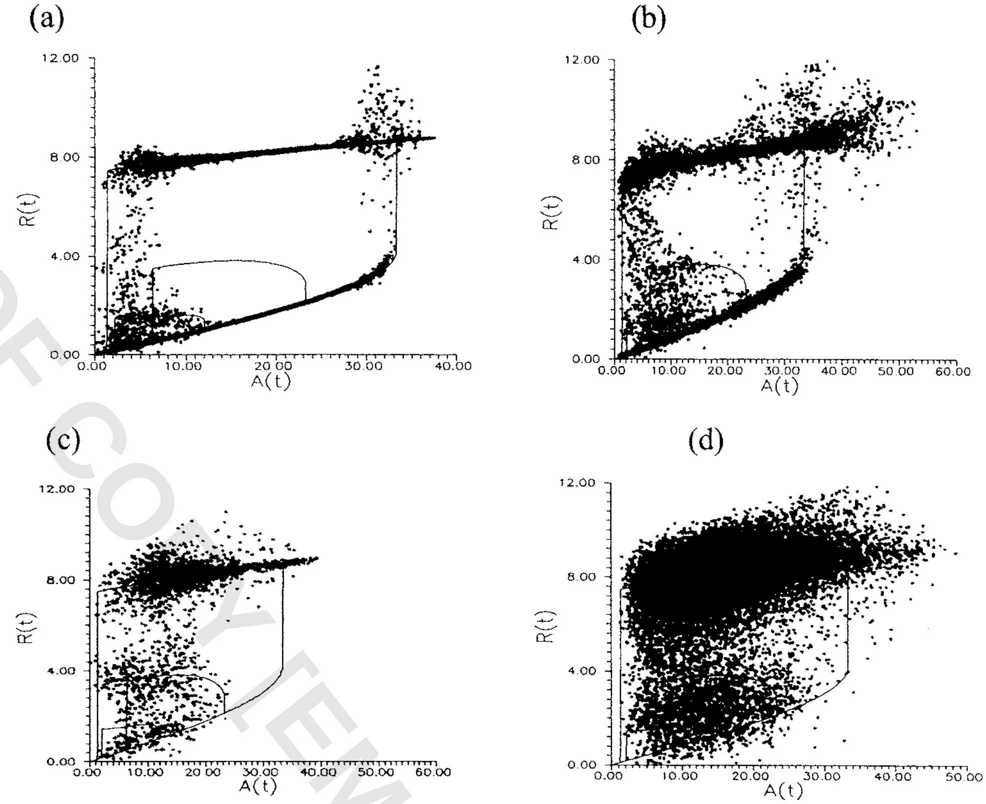

Fig. 4. (a), (b), (c), and (d) Amplitude response maps corresponding to times series shown in Figs. 3(a–d), respectively

strated in Fig. 3. As the degree of randomness in the excitation increases (increasing excitation bandwidth parameter γ), the response time series exhibits more frequent amplitude jumps among attraction domains. In addition, the total times of the response in large-amplitude primary resonance also increases. Consequently, the attraction–domain transition probability and the response–amplitude perturbation probability density functions (PDF) are related to the excitation bandwidth. As shown in the corresponding response–amplitude maps (Fig. 4), increasing excitation randomness also results in spreading of the response–amplitude distribution around the deterministic analytical response–amplitude curves.

Effect of Varying Excitation Intensity

By reducing the variance of the excitation process, the total time of the system response in the small-amplitude primary-resonance domain increases as shown in Fig. 5. The excitation bandwidth parameter employed is fixed in these cases, and thus the degree of randomness in the excitation shows no significant change. Consequently, the frequency of the response–amplitude jumps is approximately unchanged. However, the system response remains longer in the lower-amplitude primary-resonance domain in every visit with decreasing excitation variance. That is, the probability of the system response in the lower-amplitude primary-resonance domain increases as the excitation intensity (variance) decreases. Therefore, the response attraction–domain transition probability is affected by the excitation intensity. Note that in the response–amplitude maps shown in Fig. 6, the density of the points in the lower part increase as the excitation intensity decreases. Variations in the density of the response–amplitude maps also demonstrate the influence of varying excitation variance on the system response.

Predictions of Stochastic System Response Behavior

To verify the prediction capability of the proposed semianalytical method in characterizing the stochastic system response behavior in the primary and subharmonic resonance regions described above, analytical prediction of the system response in five cases, (i)–(v), with various excitation parameter sets (see Table 1) are presented and compared to simulation results.

The system damping parameter, c_s, and the linear and nonlinear restoring force parameter, a_1 and a_3, respectively, are held constant for these cases. To isolate the effects of varying the degree of excitation randomness on the response behavior, the excitation bandwidth parameter γ is increased from cases (i) to (iv), while the excitation intensity (variance) is fixed.

Effects of Varying Excitation Randomness on Attraction–Domain Transition

The system response behavior under increasing degree of excitation randomness (i.e., increasing bandwidth parameter γ), with constant excitation intensity, σ_f^2, is investigated in cases (i)–(iv). For these four cases, the normalized parameters $\rho' = |\rho|/\sigma_f^2$ and $\lambda' = |\lambda|/\sigma_f^2$, the attraction–domain probability transition matrices K, and the normalized eigenvectors corresponding to the

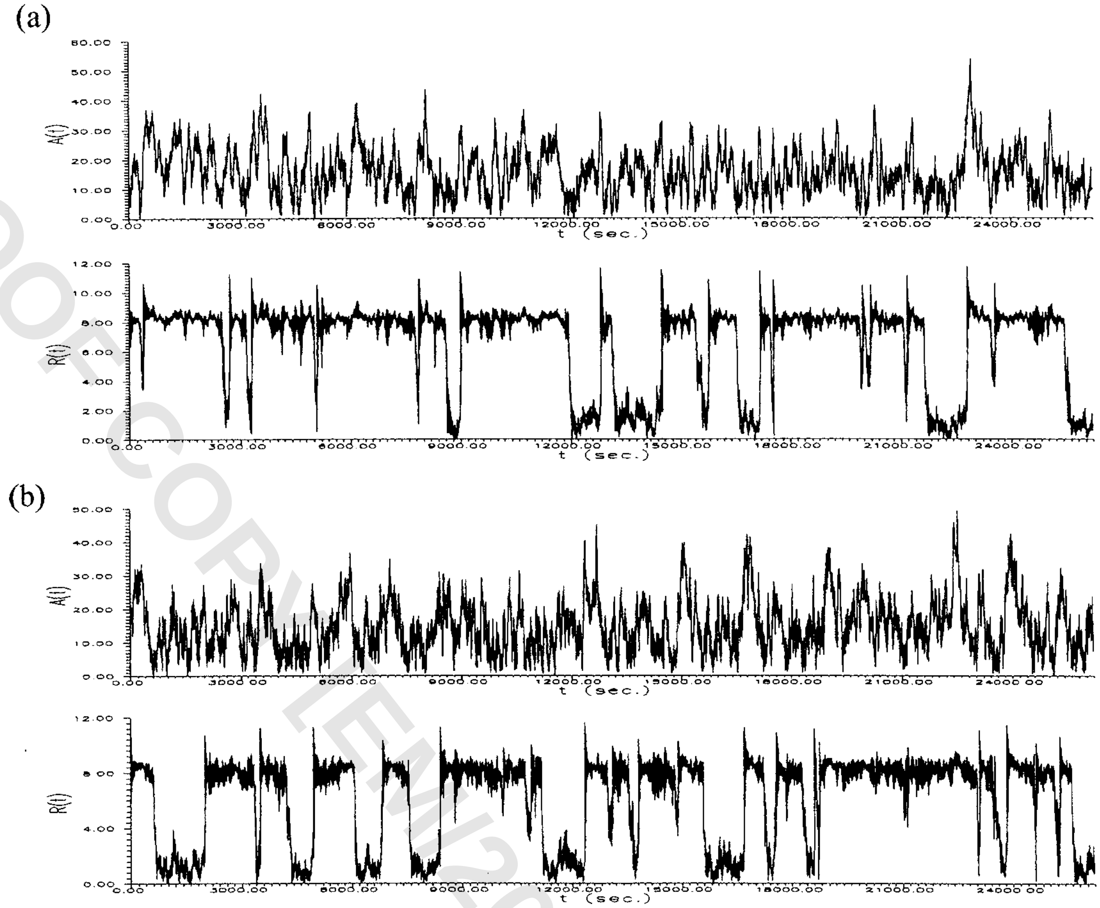

Fig. 5. (a and b) System response under varying excitation variance in subharmonic resonance region. Time series of narrowband excitation (top) and corresponding response amplitude (bottom) [c_s=0.05, a_1=1, a_3=0.3, ω_f=3.6, γ=0.01, σ_f^2=(a) 157; (b) 125].

unit eigenvalues are listed in Table 2. Note that ρ' and λ' are the normalized autocorrelation and cross-correlation, respectively, of the cosine and sine components of the excitation envelop process with a time lag equal to the central excitation period (Ochi 1990).

It is observed that the autocorrelation ρ' decreases and cross-correlation λ' increases as the excitation bandwidth parameter γ increases. Thus, the randomness in the processes of excitation amplitude cosine and sine components is increased as expected. As a result, the randomness in the excitation amplitude and phase angle increases with the excitation bandwidth. Therefore, the dependency of the stochastic behavior of the excitation parameters on γ is confirmed.

In the attraction–domain transition matrix K, as the excitation randomness parameter γ increases, the decreasing values of diagonal elements indicate increasing probability of the response exiting the current attraction domain. The off-diagonal elements, except for the zero entries and $p(4|1)$, are increasing, albeit at different rates with increasing degree of excitation randomness. That is, the probability that an attraction domain becomes the

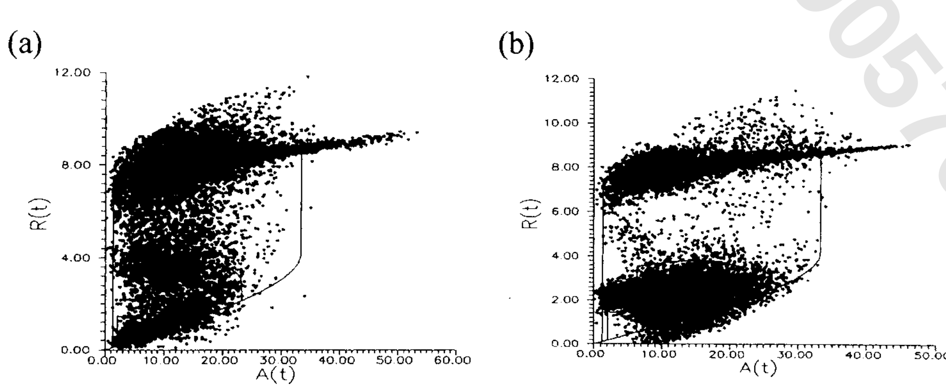

Fig. 6. (a and b) Amplitude response maps corresponding to times series shown in Figs. 5(a and b), respectively

PROOF COPY [EM/2005/024239] 005701QEM

Table 1. Parameters of System Considered in Subharmonic Resonance Region

Case	(i)	(ii)	(iii)	(iv)	(v)
System parameters			$Cs=0.05$, $a_1=1$, $a_3=0.3$		
			(a) Excitation parameters		
ω_f	3.6	3.6	3.6	3.6	3.6
γ	0.001	0.005	0.01	0.05	0.01
σ_f^2	157	157	157	157	125
			(b) Domain boundaries		
Large-amplitude harmonic domain D_1				(1.4, 50)	
Small-amplitude harmonic domain D_2				(0, 33.3)	
1/2 subharmonic domain D_3				(6.4, 23.0)	
1/3 subharmonic domain D_4				(2.2, 12.0)	

destination domain of transition from another domain increases with degree of excitation randomness. In the last column of Table 2, the probability of the response being in the large-amplitude primary resonance domain $p(D_1)$, increases with increasing bandwidth parameter γ, whereas the probability that the responses are at the lower response amplitude level (i.e., either in the small-amplitude harmonic, the 1/2 subharmonic, or the 1/3 subharmonic domains) decreases as γ increases. Thus, the trends of variation in the $p(D_d)$ observed in Table 2 agree with the stochastic response behavior described earlier. Hence, the validity of the proposed method in analyzing the response behavior under varying bandwidth parameter γ is also confirmed in the small-amplitude and subharmonic resonance regions.

Effects of Varying Excitation Randomness on Response–Amplitude Variance

To investigate the influence of varying excitation randomness on the response–amplitude variance, the variances σ_d^2 $(d=1,2,3,4)$ of the response amplitude within the attraction domains D_d^R $(d=1,2,3,4)$ are calculated from $\tilde{p}(R|D_d^R)$ $(d=1,2,3,4)$. The results obtained from cases (i)–(iv) are tabulated in Table 3. Observe that the predicted σ_d^2 $(d=1,2,3,4)$ increases with increasing excitation bandwidth parameter γ in all four coexisting attraction domains, which is consistent with the response behavior observed earlier in Fig. 3. In addition, σ_d^2 $(d=1,2,3,4)$ varies with attraction domains, reflecting the domain dependency of the system response characteristics. Therefore, the predicted trends of the response–amplitude variance of the nonlinear system under varying excitation bandwidth parameter γ by the proposed semi-analytical method are also validated.

Effects of Varying Excitation Intensity on Attraction–Domain Transition

The effects of varying excitation intensity (i.e., variance σ_f^2) on the system response behavior are investigated in cases (iii) and

Table 2. Effects of Varying Excitation Bandwidth on Response Attraction–Domain Transition Probability in Primary and Subharmonic Resonance Regions

Case	γ	ρ'	λ'	Transition matrix, K	Normalized eigenvector
(i)	0.001	0.999	0.00011	$\begin{bmatrix} 0.9977 & 0.0014 & 0.0014 & 0 \\ 0.0005 & 0.9986 & 0.0116 & 0.0385 \\ 0.0001 & 0 & 0.9802 & 0.0008 \\ 0.0015 & 0 & 0.0068 & 0.9607 \end{bmatrix}$	$\begin{Bmatrix} p(D_1) \\ p(D_2) \\ p(D_3) \\ p(D_4) \end{Bmatrix} = \begin{Bmatrix} 0.399 \\ 0.586 \\ 0.001 \\ 0.014 \end{Bmatrix}$
(ii)	0.005	0.996	0.00056	$\begin{bmatrix} 0.9959 & 0.0031 & 0.0039 & 0 \\ 0.0006 & 0.9969 & 0.0143 & 0.0742 \\ 0.0004 & 0 & 0.9566 & 0.0098 \\ 0.0031 & 0 & 0.0252 & 0.961 \end{bmatrix}$	$\begin{Bmatrix} p(D_1) \\ p(D_2) \\ p(D_3) \\ p(D_4) \end{Bmatrix} = \begin{Bmatrix} 0.426 \\ 0.547 \\ 0.009 \\ 0.018 \end{Bmatrix}$
(iii)	0.010	0.992	0.00112	$\begin{bmatrix} 0.9949 & 0.0031 & 0.0063 & 0 \\ 0.0008 & 0.9956 & 0.0195 & 0.0949 \\ 0.0017 & 0 & 0.939 & 0.0216 \\ 0.0026 & 0 & 0.0352 & 0.8835 \end{bmatrix}$	$\begin{Bmatrix} p(D_1) \\ p(D_2) \\ p(D_3) \\ p(D_4) \end{Bmatrix} = \begin{Bmatrix} 0.462 \\ 0.504 \\ 0.018 \\ 0.016 \end{Bmatrix}$
(iv)	0.050	0.958	0.00549	$\begin{bmatrix} 0.9935 & 0.0097 & 0.0183 & 0 \\ 0.001 & 0.9903 & 0.0389 & 0.1532 \\ 0.0047 & 0 & 0.8679 & 0.0846 \\ 0.0008 & 0 & 0.0749 & 0.7622 \end{bmatrix}$	$\begin{Bmatrix} p(D_1) \\ p(D_2) \\ p(D_3) \\ p(D_4) \end{Bmatrix} = \begin{Bmatrix} 0.608 \\ 0.352 \\ 0.029 \\ 0.011 \end{Bmatrix}$

Table 3. Effects of Varying Excitation Bandwidth Parameter γ on Variance of Response Amplitude within Coexisting Attraction Domains D_d^R $(d=1,2,3,4)$, Respectively, in Primary and Subharmonic Resonance Regions

	Variance σ_d^2 of response amplitude within attraction domain			
Cases	(i)	(ii)	(iii)	(iv)
γ	0.001	0.005	0.010	0.050
σ_1^2	0.0883	0.1623	0.2370	1.8192
σ_2^2	0.4738	0.5364	0.9796	2.1156
σ_3^2	0.4489	0.6716	0.8203	1.6155
σ_4^2	0.0397	0.1100	0.1885	0.8431

(v). For these two cases, the value of normalized parameter ρ' and λ' (auto- and cross-correlation coefficients), the attraction–domain transition probability matrices K, and the normalized eigenvectors corresponding to the unit eigenvalues are listed in Table 4.

As shown in Table 4, little changes in the values of ρ' and λ' are observed when the excitation variance σ_f^2 decreases from cases (iii) to (v). Thus, the randomness in the excitation is not significantly affected by the variations in the excitation intensity but the behavior of the excitation amplitude still depends on the excitation variance. In the transition matrices K, the complexity of the transition behavior is reflected by the variations in the off-diagonal elements. Under complex response attraction–domain transitions (global bifurcation), the trends of variations in the probabilities of the response in the higher and lower amplitude levels, respectively, is still accurately predicted as shown in the last column of Table 4. That is, $p(D_1)$ decreases but $\Sigma p(D_i)$ $(i=2,3,4)$ increases with decreasing excitation variance σ_f^2. This result agrees with the response characteristics observed in the previous section.

Effects of Varying Excitation Randomness on Response–Amplitude Distribution

As the degree of excitation randomness (i.e., bandwidth parameter γ) increases from cases (i) to (iv), Fig. 7 shows that the response–amplitude probability mass in the higher level increases in accordance with the response behavior observed earlier. In case (iv), although the simulations appear to show only a single mode located in the higher amplitude level in the probability distribution, the long tail of the distribution in the lower amplitude level indicates the existence of a less obvious mode in that region. The less consistent match in the results of case (iv) in the lower amplitude level is probably due to insufficient samples in that region. The comparisons of predictions with simulations for cases (i), (ii), (iii), and (iv) are shown in Fig. 8. Observe that the semianalytical method predicts well the stochastic dependency of the small- and large-amplitude responses on excitation bandwidth parameter γ.

Effects of Varying Excitation Intensity on Response–Amplitude Distribution

As the excitation variance, σ_f^2, decreases from cases (iii) to (v), Fig. 9 shows that the response–amplitude probability mass in the higher level decreases in accordance with the response behavior described earlier. By the proposed semianalytical method, the same trend of variations in the response amplitude probability distribution due to changes in excitation variance is captured as shown in Fig. 9.

Comparisons with Existing Analytical Methods

Stochastic Averaging Method

According to Rajan and Davies (1988); Davies and Liu (1990); and Koliopulos and Bishop (1993), the suggested form of the response–amplitude probability distribution can be expressed as

$$p(y) = C\exp\left\{\frac{-2\nu^2\delta}{(\varepsilon+\delta)\eta}y\left[(\varepsilon+\delta)^2+\frac{(\nu^2-1)^2}{4\nu^2} - \frac{3(\nu^2-1)y}{16\nu^2}+\frac{9y^2}{192\nu^2}\right]\right\} \quad (1)$$

and

$$y=\frac{a_3}{a_1}R^2,\quad \delta=\frac{s_C}{2\sqrt{a_1}},\quad \eta=\frac{a_3}{a_1^3}\sigma_f^2,\quad \varepsilon=\frac{\gamma}{2\sqrt{a_1}},\quad \nu=\frac{\omega_f}{\sqrt{a_1}} \quad (2)$$

where R=response amplitude; c_s, a_1, and a_3=structural damping, linear stiffness, and nonlinear stiffness coefficients, respectively; and as previously defined, γ, ω_f, and σ_f^2=excitation bandwidth parameter, central frequency, and variance, respectively.

Table 4. Effects of Varying Excitation Variance on Response Attraction–Domain Transition Probability in Primary and Subharmonic Resonance Regions

Case	σ_f^2	ρ'	λ'	Transition matrix, K	Normalized eigenvector
(iii)	157	0.992	0.00112	$\begin{bmatrix}0.9949 & 0.0031 & 0.0063 & 0\\0.0008 & 0.9956 & 0.0195 & 0.0949\\0.0017 & 0 & 0.939 & 0.0216\\0.0026 & 0 & 0.0352 & 0.8835\end{bmatrix}$	$\begin{Bmatrix}p(D_1)\\p(D_2)\\p(D_3)\\p(D_4)\end{Bmatrix}=\begin{Bmatrix}0.462\\0.504\\0.018\\0.016\end{Bmatrix}$
(v)	125	0.997	0.00113	$\begin{bmatrix}0.9936 & 0.0021 & 0.0040 & 0\\0.0010 & 0.9979 & 0.0138 & 0.0894\\0.0015 & 0 & 0.946 & 0.0155\\0.0039 & 0 & 0.0362 & 0.8951\end{bmatrix}$	$\begin{Bmatrix}p(D_1)\\p(D_2)\\p(D_3)\\p(D_4)\end{Bmatrix}=\begin{Bmatrix}0.243\\0.733\\0.011\\0.013\end{Bmatrix}$

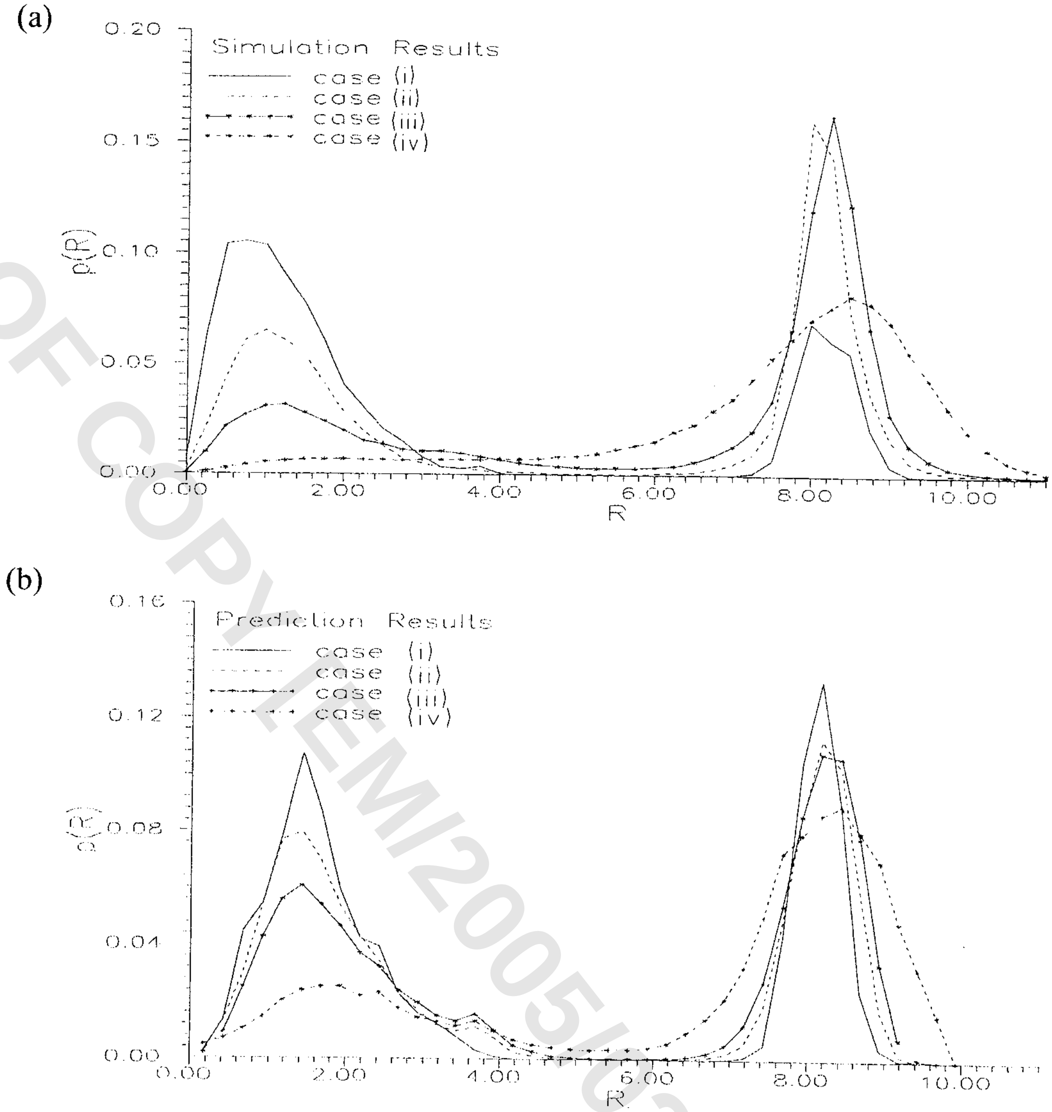

Fig. 7. Variations in response amplitude probability distribution under varying excitation bandwidth parameter γ in subharmonic resonance region: (a) simulation; (b) prediction

Quasi-Harmonic Method

From Koliopulos and Bishop (1993) the relationship between the narrow band excitation amplitude A and the corresponding response amplitude R is obtained as

$$y^3+\frac{8}{3}(1-\nu^2)y^2+\frac{16}{9}[(1-\nu^2)^2+4\delta^2\nu^2 y]=\frac{32}{9}\theta, \quad \theta=\frac{A^2 a_3}{2a_1^3} \tag{3}$$

where the scaled parameters y, δ, and ν are defined in Eq. (2). The response–amplitude probability distribution can be obtained by a probability transformation rule between the random variable θ and y through the functional relationship defined in Eq. (3) (Ochi 1990). The PDF of θ is obtained as (Koliopulos and Bishop 1993)

$$p(\theta)=\frac{1}{\eta}e^{(\theta/\eta)}, \quad \eta=\frac{a_3\sigma_f^2}{a_1^3} \tag{4}$$

Since Eq. (3) is a third-degree polynomial equation, for a given θ, there may exist three real solutions, with the smallest and the largest magnitudes correspond to the coexisting stable (physically observable) small and large amplitude steady-state responses. The real intermediate magnitude solution, associated with the unstable steady-state response, is physically unrealizable. In this case, the probability mass associated with θ will be transferred and distributed to the smallest and the largest values of y, respectively, by a ratio κ determined by the following equation (Dimentberg 1971, 1988; Koliopulos et al. 1991; Koliopulos and Bishop 1993; Koliopulos and Langley 1993)

$$\kappa=\frac{\mathrm{Ei}\left(\frac{\theta_{\max}}{\eta}\right)-\mathrm{Ei}\left(\frac{\theta_{\min}}{\eta}\right)}{\ln\left(\frac{\theta_{\max}}{\theta_{\min}}\right)}-1, \quad \mathrm{Ei}(x)=\int_{-\infty}^{x}\frac{e^{\nu}}{\nu}d\nu \tag{5}$$

where $\theta_{\max}$ and $\theta_{\min}$=respective upper and lower bounds of θ, which corresponds to multiple solutions of Eq. (1).

Comparisons of Analytical Predictions and Simulation Results

The prediction capabilities of the proposed semianalytical method developed earlier and the stochastic averaging method presented

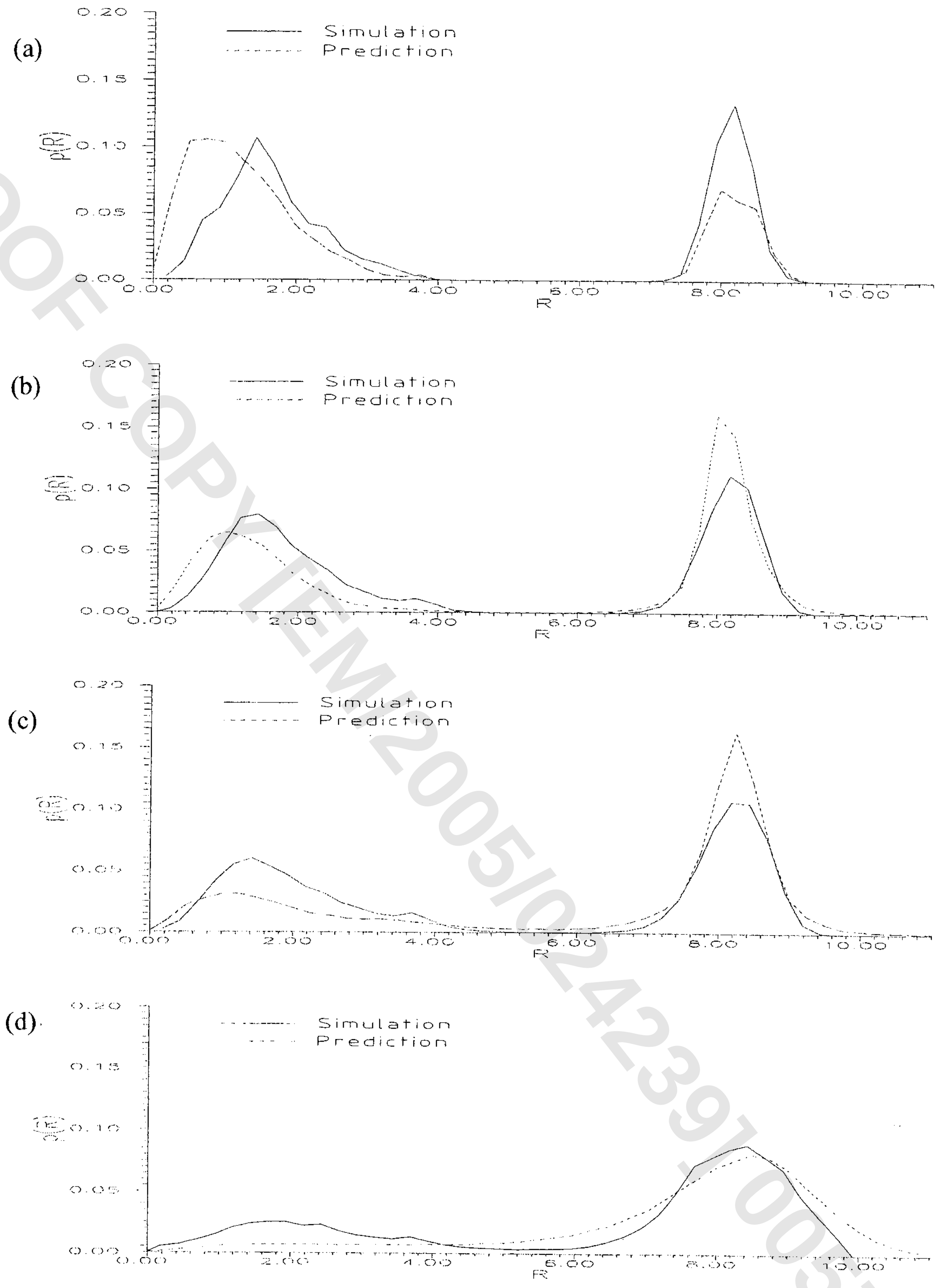

Fig. 8. Variations in response amplitude probability distribution under varying excitation bandwidth parameter γ in subharmonic resonance region: (a) case (i); (b) case (ii); (c) case (iii); and (d) case (iv)

321 by Davies and Liu (1990) and the quasi-harmonic method
322 presented by Koliopulos and Bishop (1993) are examined. In
323 particular, the response–amplitude probability distributions pre-
324 dicted by these methods for two specific excitation bandwidths
325 selected by Koliopulos and Bishop (1993) are compared. In both
326 cases, (a) and (b), the system and the excitation parameters are:
327 (c_s=0.16, a_1=1, a_3=0.3, ω_f=2, γ=0.01, σ_f^2=3.05), whereas, the
328 excitation bandwidth parameter are γ=0.02, and 0.08, re-
spectively. Note that corresponding to these system and excita- 329
tion parameters, the scaled parameters employed in the stochastic 330
averaging and the quasi-harmonic methods are [ν=2, δ=0.08, 331
$\varepsilon=\gamma/(2\sqrt{a1})$=0.01, η=0.91] and (ν=2, δ=0.08, ε=0.04, 332
η=0.91), respectively. 333

Prediction results of the semianalytical, stochastic, averaging, 334
and quasi-harmonic methods are shown in Fig. 10(a) for case (a) 335

PROOF COPY [EM/2005/024239] 005701QEM

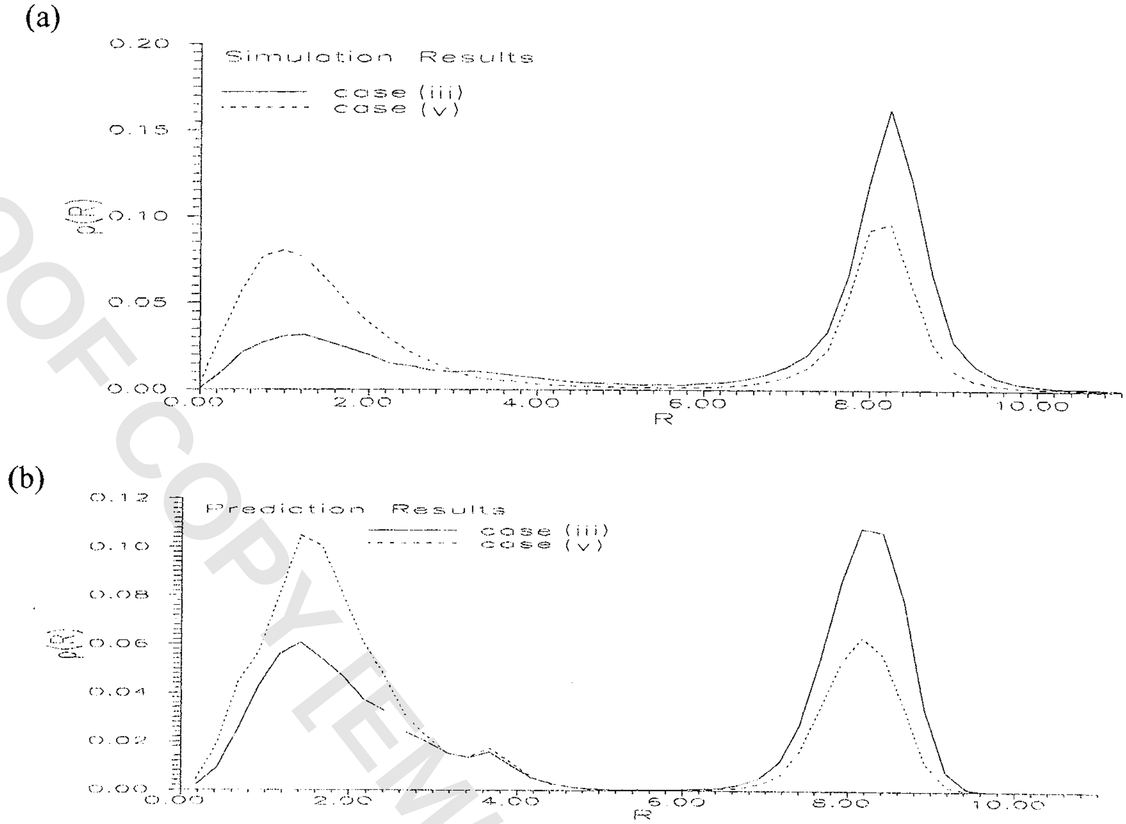

Fig. 9. Variations in response amplitude probability distribution under varying excitation variance, σ_f^2, in subharmonic resonance region: (a) simulation; (b) prediction

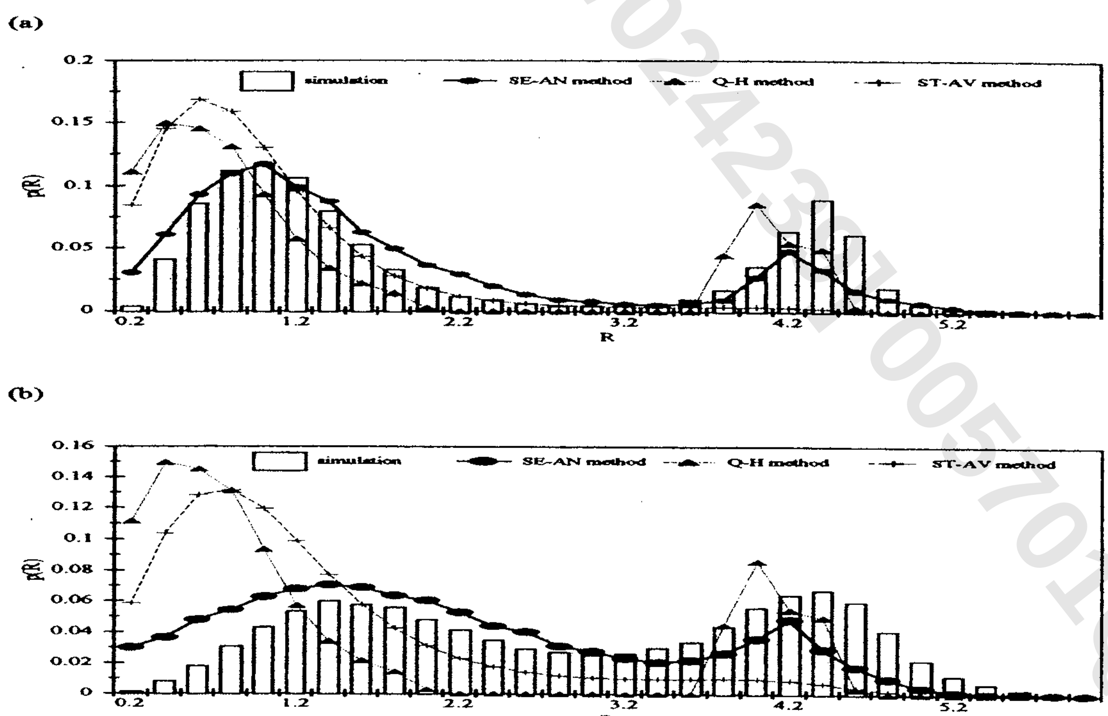

Fig. 10. Response amplitude histogram and probability distributions predicted by semi-analytical (SE-AN), quasi-harmonic (QH), and stochastic averaging (ST-AV) methods, respectively (c_s=0.16, a_1=1, a_3=0.3, ω_f=2, σ_f^2=3.05): (a) γ=0.02; (b) γ=0.08

PROOF COPY [EM/2005/024239] 005701QEM

and Fig. 10(b) for case (b). Comparisons are also made with the response amplitude histogram obtained from simulations conducted through the method described earlier. Observe that among the analytical prediction methods, the one proposed in this study agrees best with simulation results.

Concluding Remarks

Based on the results of this study, the following concluding remarks are offered: The proposed semianalytical method is capable of accurately characterizing the stochastic response behavior of the nonlinear system subject to narrowband excitations by predicting the response–amplitude probability distribution and capturing the trends of variations in the response–amplitude statistical properties. In both the primary and the subharmonic resonance regions, good agreements between the response–amplitude probability distributions predicted by the semianalytical method and obtained from simulation results are observed both qualitatively and quantitatively. In addition, trends of the variations in the probability masses associated with the modes with variations in excitation parameters (bandwidth and variance) are captured.

The analysis of the response behavior under narrowband excitations has been successfully extended to the primary and subharmonic resonance regions. In previous studies, analytical methods can only predict the response behavior in the primary resonance region where only two attraction domains coexist. In this study, we have demonstrated the capability of the proposed semianalytical method in predicting more complex response behavior in the primary and subharmonic resonance regions where four attraction domains coexist.

A significant improvement in the accuracy of predicting response amplitude probability distributions is achieved by the proposed semianalytical method. This is because the stochastic nonlinear response behavior under narrowband excitation is accurately characterized by the semianalytical method through modeling the response attraction–domain transition and response–amplitude perturbations.

Acknowledgments

Financial support from the U.S. Office of Naval Research (Grant Nos. N00014-92-J-1221 and N00014-04-10008) is gratefully acknowledged.

References

Davies, H. G., and Liu, Q. (1990). "The response envelope probability density function of a Dulling oscillator with random narrow-band excitation." *J. Sound Vib.*, 139, 1–8.

Davies, H. G., and Nandlall, D. (1986). "Phase plane for narrow-band random excitation of a duffing oscillator." *J. Sound Vib.*, 104, 277–283.

Davies, H. G., and Rajan, S. (1988). "Random superharmonic and subharmonic response: Multiple time scaling of a duffing oscillator." *J. Sound Vib.*, 26, 195–208.

Dimentberg, M. F. (1971). "Oscillations of a system with nonlinear cubic characteristics under narrow band random excitation." *Mech. Solids*, 6, 142–146.

Dimentberg, M. F. (1988). *Statistical dynamics of nonlinear and time-varying systems*, Wiley, New York.

Francescutto, A. (1991). "On the probability of large amplitude rolling and capsizing as a consequence of bifurcations." *Proc., Int. Conf. on Offshore Mechanics and Arctic Engineering*, Vol. II, 91–96.

Guckenheimer, J., and Holmes, P. (1986). *Nonlinear oscillations, dynamical systems, and bifurcation of vector fields*, Springer, New York.

Koliopulos, P. K., and Bishop, S. R. (1993). "Quasiharmonic analysis of the behavior of a hardening dulling oscillator subjected to filtered white noise." *Nonlinear Dyn.*, 4, 279–288.

Koliopulos, P. K., Bishop, S. R., and Stefanou, G. D. (1991). "Response statistics of nonlinear system under variations of excitation bandwidth." *Computational stochastic mechanics*, Vol. 33, Elsevier Applied Science, London, 5–348.

Koliopulos, P. K., and Langley, R. S. (1993). "Improved stability analysis of the response of a duffing oscillator under filtered white noise." *Int. J. Non-Linear Mech.*, 28, 145–155.

Lin, H., and Yim, S. C. S. (1997). "Noisy nonlinear motions of moored systems. Part 1: Analysis and simulation." *J. Waterway, Port, Coastal, Ocean Eng.*, 123(5), 285–295.

Nayfeh, A. H., and Mook, D. T. (1979). *Nonlinear oscillations*, Wiley, New York.

Ochi, M. K. (1990). *Applied probability and stochastic processes in engineering and physical sciences*, Wiley, New York.

Rajan, S., and Davies, H. G. (1988). "Multiple time scaling of the response of a Duffing oscillator to narrow-band random excitation." *J. Sound Vib.*, 123, 497–506.

Roberts, J. B., and Spanos, P. D. (1986). "Stochastic averaging: An approximate method of solving random vibration problems." *Int. J. Non-Linear Mech.*, 21, 111–134.

Shinozuka, M. (1971). "Simulation of multivariate and multidimensional random processes." *J. Acoust. Soc. Am.*, 49, 357–367.

Shinozuka, M., and Deodatis, G. (1991). "Simulation of stochastic processes by spectral representation." *Appl. Mech. Rev.*, 44(4), 191–203.

Yim, S. C., Yuk, D., Naess, A., and Shih, I. M. (2006). "Global and local nonlinear system responses under narrowband random excitations, Part I: Semianalytical method." *J. Eng. Mech.*, submitted for publication.

PROOF COPY [EM/2005/024239] 005701QEM